Continuous-variable dense coding by optomechanical cavities

Shabir Barzanjeh,[1] Stefano Pirandola,[2] and Christian Weedbrook[3]
[1]*Institute for Quantum Information, RWTH Aachen University, 52056 Aachen, Germany*
[2]*Department of Computer Science, University of York, York YO10 5GH, United Kingdom*
[3]*Department of Physics, University of Toronto, Toronto M5S 3G4, Canada*
(Received 7 August 2013; published 25 October 2013)

In this paper, we show how continuous-variable dense coding can be implemented using entangled light generated from a membrane-in-the-middle geometry. The mechanical resonator is assumed to be a high reflectivity membrane hung inside a high quality factor cavity. We show that the mechanical resonator is able to generate an amount of entanglement between the optical modes at the output of the cavity, which is strong enough to approach the capacity of quantum dense coding at small photon numbers. The suboptimal rate reachable by our optomechanical protocol is high enough to outperform the classical capacity of the noiseless quantum channel.

DOI: 10.1103/PhysRevA.88.042331 PACS number(s): 42.50.Ex, 03.67.Lx, 42.50.Wk, 85.85.+j

I. INTRODUCTION

The entanglement of quantum states plays an important role in quantum information [1]. Sharing an entangled quantum state, such as an Einstein-Podolsky-Rosen (EPR) state [2], makes it possible to perform quantum communication processes like quantum dense coding [3], quantum teleportation [4], quantum cryptography [5], and quantum computational tasks [6]. The experimental realizations of these protocols have been achieved in several physical systems, such as photons, trapped ions, atoms in optical lattices, nuclear magnetic resonance, etc. [7,8].

A wide range of theoretical and experimental schemes have been also proposed to generate, observe, and/or exploit entanglement using macroscopic objects [9–25]. Very recently, it has been shown how mechanical resonators can be used as a novel tool for generating strong continuous-variable (CV) entanglement [26], which may involve optical modes at different wavelengths [22,27,28]. Such strong CV entanglement can therefore be exploited to implement quantum information tasks, like dense coding as studied in this paper.

Quantum dense coding, originally proposed for qubits [3], provides a method by which two bits of information can be transmitted by sending only one qubit, provided that an entangled resource was previously shared by the parties. This idea was then extended to the CV setting where the rate at which information is transmitted can potentially be doubled by the use of EPR states as the source of the entanglement [2,29–32].

In this paper, we show how we can successfully implement the protocol of CV dense coding by exploiting the optical entanglement at the output of an optomechanical cavity with a membrane-in-the-middle geometry [33,34]. This system consists of a high finesse cavity with two fixed-end mirrors and a perfectly reflecting movable middle mirror, such as a dielectric membrane. We show the ability of the mechanical resonator to generate strong entanglement between two output optical beams, in a way which is robust with respect to the various optomechanical parameters, like the cavity damping rates, the laser input powers and bandwidths, and the temperature of the membrane. Then, using this optical entanglement, we prove that we can perform dense coding with a rate which closely approximates the dense coding capacity at small photon numbers. We also show that this rate is good enough to outperform the (one-way) classical capacity of the noiseless quantum channel.

The paper is structured as follows. In Sec. II, we first give a thorough theoretical description of the system under consideration and the quantum Langevin equations (QLEs) are derived and linearized around the semiclassical steady state. In Sec. III, we study the steady state of the system and quantify the entanglement between the output optical modes by using the logarithmic negativity. Note that most of the contents of these two sections are a review of previous literature (for instance, see Ref. [35] and references therein) which is given to the reader for the sake of completeness. Then, in Sec. IV, there are the main results of our paper. Here we show that the optomechanical source is able to approach the capacity of dense coding at low energies, and to outperform the classical capacity of the noiseless quantum channel at higher energies. Finally, our conclusions are given in Sec. V.

II. DESCRIPTION AND DYNAMICS OF THE OPTOMECHANICAL SYSTEM

We start with a sketch of the system as shown in Fig. 1. A perfectly reflecting membrane with mass m is placed in the middle of a cavity formed by two fixed mirrors separated from each other by a distance $2L$. Two strong coupling fields with amplitudes ϵ_r and ϵ_l and frequencies ω_{0r} and ω_{0l}, respectively, are sent into the cavity through the partially transmitting right and left mirrors. The right and left subcavities are assumed to be linearly coupled to the displacement of the membrane with coupling constants G_{0r} and G_{0l}, respectively. Hence the system's time-dependent Hamiltonian takes the form [36]

$$\begin{aligned} H =& \hbar\omega_r a^\dagger a + \hbar\omega_l b^\dagger b + \frac{\hbar\Omega_m}{2}(p^2+q^2) \\ &+ \hbar(G_{0r}a^\dagger a - G_{0l}b^\dagger b)q + i\hbar\epsilon_r(a^\dagger e^{-i\omega_{0r}t} - a e^{i\omega_{0r}t}) \\ &+ i\hbar\epsilon_l(b^\dagger e^{-i\omega_{0l}t} - b e^{i\omega_{0l}t}), \end{aligned} \tag{1}$$

where a (b) is the annihilation operator for right (left) subcavity photon with resonance frequency $\omega_r(\omega_l)$, while q and p ($[q,p]=i$) are the dimensionless position and momentum operators of the membrane with frequency Ω_m. In Eq. (1), the

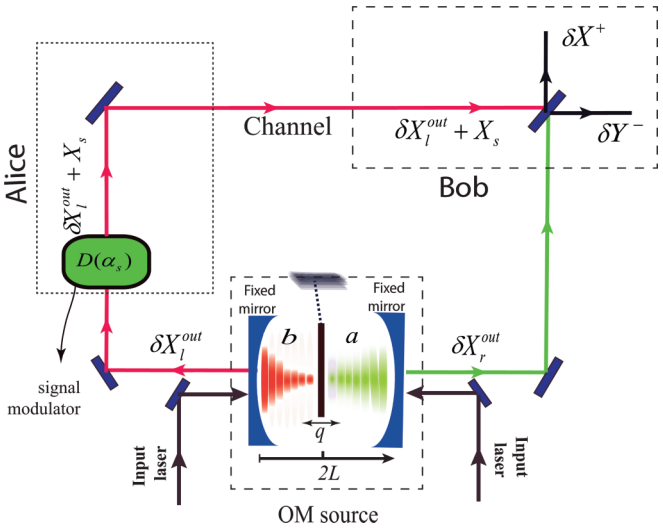

FIG. 1. (Color online) Protocol of continuous-variable dense coding equipped with an optomechanical (OM) device as the source of the entanglement. The preparation of the entanglement consists of a perfectly reflecting movable middle mirror dividing the cavity into two separated subcavities right and left with intracavity modes a and b, respectively. The subcavities are excited by two lasers through fixed mirrors. The left l and right r optical outputs of the subcavities are entangled and used to implement continuous-variable dense coding.

optomechanical coupling constants are expressed by $(i = r,l)$

$$G_{0i} = \omega_i/L\sqrt{\hbar/m\Omega_m}$$

and

$$\epsilon_i = \sqrt{2P_i\kappa_i/\hbar\omega_{0i}},$$

where P_i is the power of the probe lasers impinged inside the cavity through the right and left mirrors, and κ_i are the damping rates of the subcavities' photons via the end mirrors.

In the rotating frame at the frequencies ω_{0r} and ω_{0l} of the driven lasers, we can derive the QLEs for the mirror and the subcavities variables [37]

$$\begin{aligned}
\dot{q} &= \Omega_m p,\\
\dot{p} &= -\Omega_m q - \gamma_m p - G_{0r}a^\dagger a + G_{0l}b^\dagger b + \xi,\\
\dot{a} &= -(\kappa_r + i\Delta_{0r})a - iG_{0r}qa + \epsilon_r + \sqrt{2\kappa_r}a_{\rm in},\\
\dot{b} &= -(\kappa_l + i\Delta_{0l})b + iG_{0l}qb + \epsilon_l + \sqrt{2\kappa_l}b_{\rm in},
\end{aligned} \tag{2}$$

where $\Delta_{0i} = \omega_i - \omega_{0i}$ are the detunings, γ_m is the mechanical damping rate, $a_{\rm in}(t)$ and $b_{\rm in}(t)$ are subcavities' input noises, and $\xi(t)$ is the Brownian noise acting on the mechanical resonator, with correlation function [35,38]

$$\langle\xi(t)\xi(t')\rangle = \frac{\gamma_m}{\Omega_m}\int\frac{d\omega}{2\pi}e^{-i\omega(t-t')}\omega\left[\coth\left(\frac{\hbar\omega}{2k_BT}\right)+1\right], \tag{3}$$

with k_B being the Boltzmann constant, and T the temperature of the reservoir.

In a very high mechanical quality factor regime, i.e., for $Q = \Omega_m/\gamma_m \to \infty$, the mechanical noise is characterized by white thermal noise [39]:

$$\langle\xi(t)\xi(t') + \xi(t')\xi(t)\rangle/2 \simeq \gamma_m(2\bar{n}+1)\delta(t-t'),$$

with mean excitation number $\bar{n} = [\exp(\hbar\Omega_m/k_BT) - 1]^{-1}$. The subcavities' input noises, $a_{\rm in}(t)$ and $b_{\rm in}(t)$, also obey white-noise correlation functions [37]

$$\begin{aligned}
\langle a_{\rm in}(t)a_{\rm in}^\dagger(t')\rangle &= \delta(t-t'), \quad \langle a_{\rm in}^\dagger(t)a_{\rm in}(t')\rangle = 0,\\
\langle b_{\rm in}(t)b_{\rm in}^\dagger(t')\rangle &= \delta(t-t'), \quad \langle b_{\rm in}^\dagger(t)b_{\rm in}(t')\rangle = 0,
\end{aligned} \tag{4}$$

where we have set $N(\omega_i) = [\exp(\hbar\omega_i/k_BT) - 1]^{-1} \approx 0$, since $\hbar\omega_i/k_BT \gg 1$ at optical frequencies.

III. STATIONARY ENTANGLEMENT OF THE OUTPUT OPTICAL MODES

In this section we study the stationary entanglement between the two optical modes at the output of the cavity. For this purpose, we derive the stationary correlation matrix of the system under consideration. First, we linearize the QLEs given in Eq. (2) around the semiclassical fixed points, i.e., $q = q_s + \delta q$, $p = p_s + \delta p$, $a = \alpha + \delta a$, and $b = \beta + \delta b$. The fixed points are obtained by setting the time derivatives to zero, resulting in

$$\begin{aligned}
p_s &= 0,\\
q_s &= \frac{G_{0l}|\beta|^2 - G_{0r}|\alpha|^2}{\Omega_m},\\
\alpha &= \frac{e^{i\pi}\epsilon_r}{\sqrt{\kappa_r + \Delta_r}},\\
\beta &= \frac{\epsilon_l}{\sqrt{\kappa_l + \Delta_l}}.
\end{aligned} \tag{5}$$

where $\Delta_r = \Delta_{0r} + G_{0r}q_s$ and $\Delta_l = \Delta_{0l} - G_{0l}q_s$ describe the effective detunings of the right and left subcavities' fields, respectively.

In the frequency domain, the stationary covariance matrix (CM) for the quantum fluctuations of the mirror and the output of optical modes' variables, $\mathbf{u}^{\rm out}(t) = [\delta q(t),\delta p(t),\delta X_l^{\rm out}(t),\delta Y_l^{\rm out}(t),\delta X_r^{\rm out}(t),\delta Y_r^{\rm out}(t)]^T$, takes the form [35]

$$\begin{aligned}
\mathbf{V}^{\rm out} &= \lim_{t\to\infty}\frac{1}{2}\langle u_i^{\rm out}(t)u_j^{\rm out}(t) + u_j^{\rm out}(t)u_i^{\rm out}(t)\rangle\\
&= \int d\omega\boldsymbol{\Upsilon}(\omega)(\tilde{\mathbf{M}}^{\rm ext}(\omega) + \mathbf{P}_{\rm out})\\
&\quad\times\mathbf{D}_{\rm ext}(\tilde{\mathbf{M}}^{\rm ext}(\omega)^\dagger + \mathbf{P}_{\rm out})\boldsymbol{\Upsilon}^\dagger(\omega),
\end{aligned} \tag{6}$$

where $\tilde{\mathbf{M}}^{\rm ext}(\omega) = (i\omega + A)^{-1}$,

$$\mathbf{A} = \begin{pmatrix}
0 & \Omega_m & 0 & 0 & 0 & 0\\
-\Omega_m & -\gamma_m & G_l & 0 & G_r & 0\\
0 & 0 & -\kappa_l & \Delta_l & 0 & 0\\
G_l & 0 & -\Delta_r & -\kappa_l & 0 & 0\\
0 & 0 & 0 & 0 & -\kappa_r & \Delta_r\\
G_r & 0 & 0 & 0 & -\Delta_r & -\kappa_r
\end{pmatrix}, \tag{7}$$

with

$$\begin{aligned}
\mathbf{P}_{\rm out} &= {\rm diag}[0,0,1/2k_l,1/2k_l,1/2k_r,1/2k_r],\\
\mathbf{D}^{\rm ext} &= {\rm diag}[0,\gamma_m(2\bar{n}_b+1),2\kappa_l,2\kappa_l,2\kappa_r,2\kappa_r],
\end{aligned}$$

and $\boldsymbol{\Upsilon}(\omega)$ is the Fourier transform of

$$\boldsymbol{\Upsilon}(t)=\begin{pmatrix}\delta(t) & 0 & 0 & 0 & 0 & 0\\ 0 & \delta(t) & 0 & 0 & 0 & 0\\ 0 & 0 & R_l & -I_l & 0 & 0\\ 0 & 0 & I_l & R_l & 0 & 0\\ 0 & 0 & 0 & 0 & R_r & -I_r\\ 0 & 0 & 0 & 0 & I_r & R_r\end{pmatrix},$$

where $G_i=\frac{2\omega_i}{L}\sqrt{\frac{P_i\kappa_i}{m\Omega_m\omega_{0i}(\kappa_i^2+\Delta_i^2)}}(i=r,l)$ are the effective optomechanical coupling constants, and $R_j=\sqrt{2\kappa_j}\mathrm{Re}[g_j(t)]$ and $I_j=\sqrt{2\kappa_j}\mathrm{Im}[g_j(t)]$ $(j=r,l)$ are determined by the causal filter functions [35,40] $g_j(t)$, with bandwidths $1/\tau_j$ and central frequencies Ω_j.

From the global CM of Eq. (6) we extract the reduced CM $\mathbf{V}'$ of the output optical modes with quadrature fluctuations $\delta X_l^{\mathrm{out}}$, $\delta Y_l^{\mathrm{out}}$, $\delta X_r^{\mathrm{out}}$, and $\delta Y_r^{\mathrm{out}}$. This matrix can be written in the block form

$$\mathbf{V}'=\begin{pmatrix}L\mathbf{I} & \mathbf{C}\\ \mathbf{C}^T & R\mathbf{I}\end{pmatrix},\quad \mathbf{C}=\begin{pmatrix}-C & C'\\ C' & C\end{pmatrix},\tag{8}$$

where $L,R\geqslant 1/2$, $C\geqslant 0$, and C' is numerically small compared with the other matrix elements. This CM completely characterizes the stationary Gaussian state of the output cavity modes. In particular, this CM approximates that of an EPR state with cross correlations of the kind $\delta X_l^{\mathrm{out}}\approx -\delta X_r^{\mathrm{out}}$ and $\delta Y_l^{\mathrm{out}}\approx \delta Y_r^{\mathrm{out}}$.

In order to study the conditions under which the output optical modes are entangled, we consider the logarithmic negativity E_N [41] given by

$$E_N=\max[0,-\ln(2\zeta)],\tag{9}$$

where ζ is the least partially transposed symplectic eigenvalue of $\mathbf{V}'$ [2,42]. This is given by

$$\zeta=\sqrt{\frac{\Lambda(\mathbf{V}')-\sqrt{\Lambda(\mathbf{V}')^2-4\det\mathbf{V}'}}{2}},\tag{10}$$

with $\Lambda(\mathbf{V}')=L^2+R^2-2\det\mathbf{C}$.

In Fig. 2 we have plotted the logarithmic negativity E_N versus the normalized frequency of the output cavity mode Ω_l/Ω_m for two different values of membrane quality factor $Q=10^4$ and $Q=15\times 10^4$. We have assumed an experimental situation [33,43] representing a membrane with vibrational frequency $\Omega_m/2\pi=10$ MHz and mass $m=10$ ng. The right side subcavity has damping rate $\kappa_r=0.4\Omega_m$ and the laser power imping on this subcavity is assumed to be $P_r=10$ mW. The left side subcavity damping rate is $\kappa_l=0.1\Omega_m$ with the laser power $P_l=48$ mW. The temperature of the membrane's reservoir is $T=1$ K and the subcavities' detunings have been fixed at $\Delta_r=-\Delta_l=-\Omega_m$ with $\Omega_r=-\Omega_m$. Figure 2 shows that the entanglement between output cavity fields is maximum around $\Omega_l=\Omega_m$. Also we see that by increasing the quality factor of the mechanical resonator one can increase the entanglement between the subcavities' output fields, as one should expect.

A more interesting situation is depicted in Fig. 3 which shows how entanglement between the output cavity fields

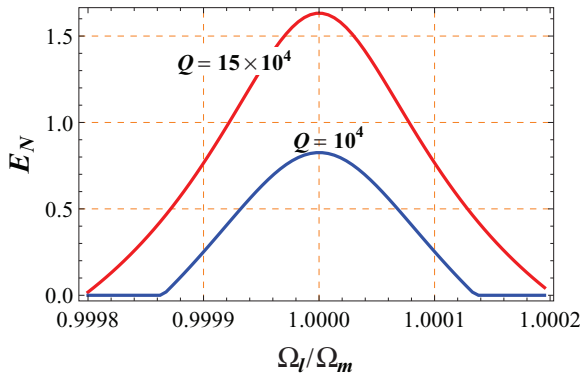

FIG. 2. (Color online) Logarithmic negativity E_N between the optical output modes of the two subcavities versus the normalized frequency Ω_l/Ω_m for two different values of the mirror's quality factor Q at a fixed temperature $T=1$ K with $\Omega_r=-\Omega_m$. The subcavities detuning have been fixed at $\Delta_r=-\Omega_m$ and $\Delta_l=\Omega_m$ while the other parameters are $\Omega_m/2\pi=10$ MHz, $\kappa_r=0.4\Omega_m$, $P_r=10$ mW, $L=1$ mm, $\kappa_l=0.1\Omega_m$, $P_l=48$ mW, and $m=10$ ng.

depends on the subcavities' damping rates. This figure shows that the entanglement reaches its maximum around $\kappa_r\sim 0.35\Omega_m$ and $\kappa_l\sim 0.2\Omega_m$, and out of this region entanglement quickly decreases. Note that the maximum of entanglement is approached around small values of damping rates which is close to the instability threshold. Finally, Fig. 4 shows the proper values of input powers which maximize entanglement. This figure reveals that by increasing the input powers one can definitely improve the entanglement between the output modes, even though at the same time the instability region is extended. Note that the generated CV entanglement can be verified from the measurement record by applying a generalized version of Duan's inequality [44].

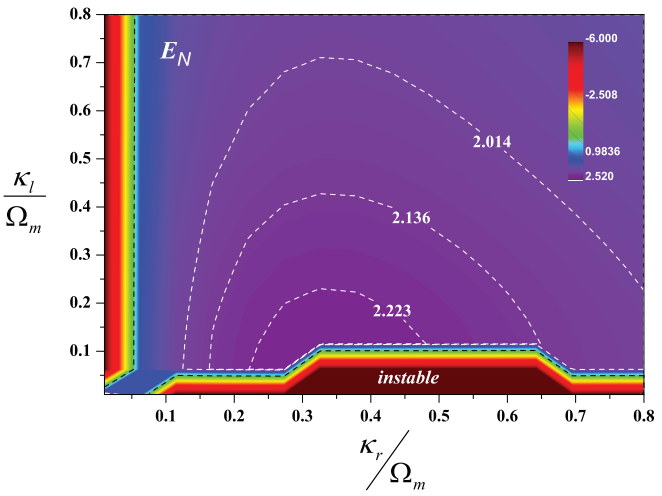

FIG. 3. (Color online) Logarithmic negativity E_N between the optical output modes of the two subcavities versus the normalized damping rates κ_l/Ω_m and κ_r/Ω_m at fixed temperature $T=1$ K and $\Omega_r=-\Omega_l=-\Omega_m$. Other parameters are the same as those in Fig. 2.

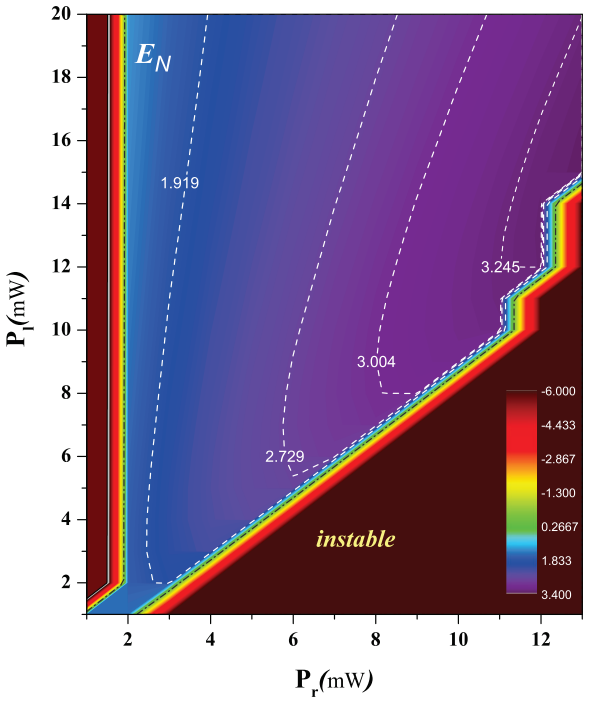

FIG. 4. (Color online) Logarithmic negativity E_N between the optical output modes of the two subcavities versus the input powers P_l and P_r for $\Omega_r = -\Omega_l = -\Omega_m$. Again the other parameters are the same as those in Fig. 2.

IV. DENSE CODING WITH AN OPTOMECHANICAL SOURCE

So far we have shown that an optomechanical cavity in the form of a membrane-in-the-middle geometry can be used to generate entanglement between two optical fields. Now we show that these optical modes are sufficiently entangled to be used for implementing the protocol of dense coding.

The scheme is the one sketched in Fig. 1, where the entangled optical beams at the output of the cavity are labeled by l and r, with mode $i = l,r$ having quadrature fluctuations $\delta X_i^{\rm out}$ and $\delta Y_i^{\rm out}$. The left mode l is sent to Alice, while the right mode r is sent to Bob. Then, Alice encodes a Gaussian complex signal $\alpha_s = (X_s + iY_s)/\sqrt{2}$ by applying the displacement operator $D(\alpha_s)$ on mode l (with V_s being the variance of each real Gaussian variable X_s and Y_s). The output mode, with quadrature fluctuations $\delta X_l^{\rm out} + X_s$ and $\delta Y_l^{\rm out} + Y_s$, is sent to Bob through a noiseless quantum channel. At his station, Bob combines the incoming signal mode with mode r in a balanced beam splitter, of which he homodynes the two output ports, measuring the position fluctuation of "+" and the momentum fluctuaction of "−". In other words, Bob detects the two operators

$$\begin{aligned} \delta X_+ &= \frac{1}{\sqrt{2}}\left(\delta X_l^{\rm out} + X_s + \delta X_r^{\rm out}\right), \\ \delta Y_- &= \frac{1}{\sqrt{2}}\left(\delta Y_l^{\rm out} + Y_s - \delta Y_r^{\rm out}\right). \end{aligned} \tag{11}$$

One can easily check that these operators have the same variance, i.e.,

$$\langle \delta X_+^2 \rangle = \langle \delta Y_-^2 \rangle = \tfrac{1}{2}(L + R - 2C + V_s) := V_B. \tag{12}$$

It is also easy to compute the conditional entropy $V_{A|B}$ which quantifies the remaining entropies of X_s and Y_s given Bob's homodyne detections. This is given by

$$\begin{aligned} V_{A|B} &= \langle X_s^2 \rangle - \frac{\langle X_s(\delta X_+)\rangle^2}{\langle \delta X_+^2 \rangle} \\ &= \langle Y_s^2 \rangle - \frac{\langle Y_s(\delta Y_-)\rangle^2}{\langle \delta Y_-^2 \rangle} = V_s - \frac{V_s^2}{2V_B}. \end{aligned} \tag{13}$$

Now, using Eqs. (12) and (13), we can compute Alice and Bob's mutual information [6,45]

$$\begin{aligned} I(A:B) &= \log_2 \frac{V_s}{V_{A|B}} \\ &= \log_2 \left(1 + \frac{V_s}{L + R + 2C}\right). \end{aligned} \tag{14}$$

Here the signal power can be written as $V_s = \bar{n}_s + 1/2$. In turn, the thermal number $\bar{n}_s$ can be written in terms of the mean number of photons $\bar{n}$ which are sent to Bob through the noiseless quantum channel. This mean photon number represents the energetic constraint of the protocol, and is equal to $\bar{n} = \bar{n}_l^{\rm out} + \bar{n}_s$, where $\bar{n}_l^{\rm out} = \langle (b_l^{\rm out})^\dagger b_l^{\rm out} \rangle$ is the average number of photons in the output cavity mode l. Then, we can write the signal power as $V_s = (\bar{n} + 1) - L$. Finally, by replacing V_s in Eq. (14) we get the mutual information of Alice and Bob $I(A:B)$ in terms of the energetic constraint $\bar{n}$.

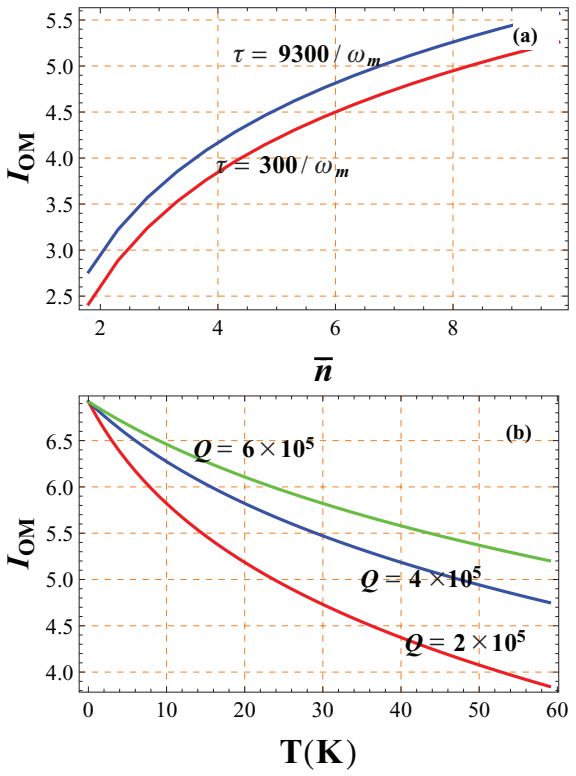

FIG. 5. (Color online) Optomechanical dense coding rate $I_{\rm OM}$ (a) versus the average photon numbers for two different values of the laser bandwidth and (b) versus the temperature of the cavity for three different values of the mirror's quality factor. Here we consider $\Omega_r = -\Omega_l = -\Omega_m$ and the other parameters are the same as in Fig. 2.

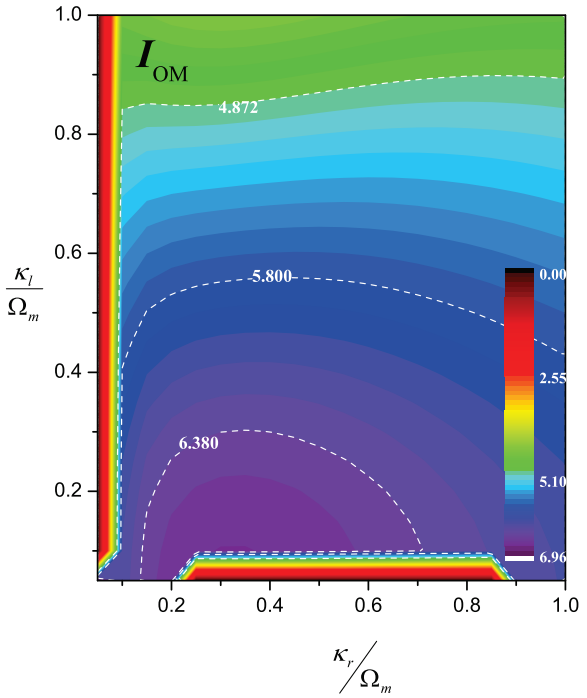

FIG. 6. (Color online) Optomechanical dense coding rate $I_{\rm OM}$ versus the normalized damping rates κ_l/Ω_m and κ_r/Ω_m at a fixed temperature $T = 1$ K and $\Omega_r = -\Omega_l = -\Omega_m$. The other parameters are the same as in Fig. 2.

This quantity represents the dense coding rate $I_{\rm OM}(\bar{n})$ which is achievable by using our optomechanical source.

In Fig. 5(a) we have plotted the optomechanical dense coding rate $I_{\rm OM}$ in terms of the energetic constraint $\bar{n}$ for two different values of laser bandwidth τ. As expected, $I_{\rm OM}$ is increasing in $\bar{n}$, and also in the bandwidth τ. Then, as shown in Fig. 5(b), we see that $I_{\rm OM}$ is relatively robust with respect to the temperature of the cavity. The dependence of the optomechanical rate on the cavity dampings is illustrated

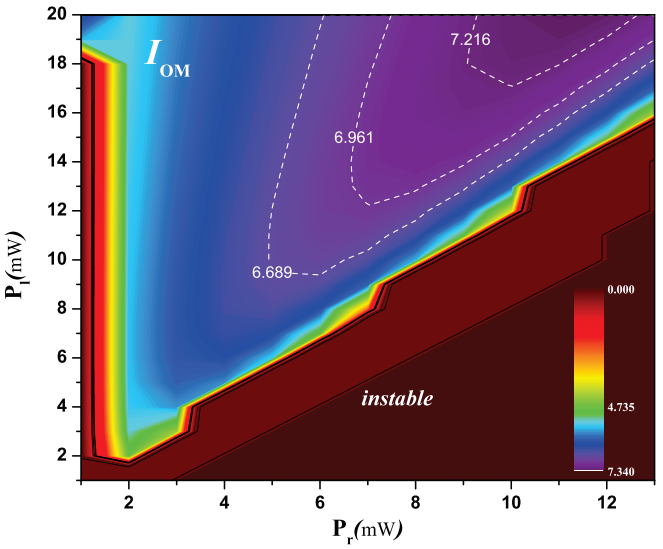

FIG. 7. (Color online) Optomechanical dense coding rate $I_{\rm OM}$ versus the input powers P_l and P_r at a fixed temperature $T = 1$ K and $\Omega_r = -\Omega_l = -\Omega_m$. The other parameters are the same as Fig. 2.

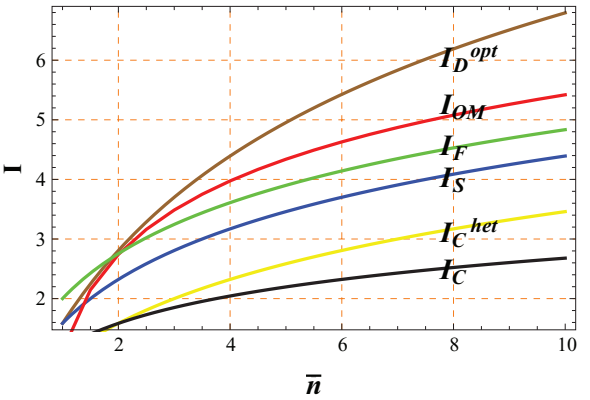

FIG. 8. (Color online) The optomechanical dense coding rate $I_{\rm OM}$ is plotted in terms of the photon number $\bar{n}$, and compared with the dense coding capacity $I_D^{\rm opt}$, the classical capacity I_F (Fock states and photon counting), the rate I_S achievable by squeezed states and homodyne, the rate $I_C^{\rm het}$ achievable by coherent states and heterodyne, and finally, the rate I_C reachable by coherent states and homodyne. We consider $T = 1$ K and $\Omega_l = -\Omega_r = \Omega_m$. The subcavities' detunings are $\Delta_l = -\Delta_r = \Omega_m$, while the other optomechanical parameters are $\Omega_m/2\pi = 10$ MHz, $\kappa_r = 0.4\Omega_m$, $P_r = 10$ mW, $L = 1$ mm, $\kappa_l = 0.1\Omega_m$, $P_l = 48$ mW, $m = 10$ ng, and $Q = 15 \times 10^4$.

in Fig. 6, where we can see that $I_{\rm OM}$ is maximum around $\kappa_r \simeq 0.25\Omega_m$ and $\kappa_l \simeq 0.1\Omega_m$. Finally, in Fig. 7 we also show the influence of the input powers.

As shown in Fig. 8, the optomechanical dense coding rate $I_{\rm OM}(\bar{n})$ is able to approximate the dense coding capacity [31] $I_D^{\rm opt}(\bar{n}) = \log_2(1 + \bar{n} + \bar{n}^2)$ for low photon numbers $\bar{n} \simeq 2$, remaining suboptimal at higher energies. As we show in the same figure, for $\bar{n} > 2$ the optomechanical dense coding rate $I_{\rm OM}(\bar{n})$ outperforms all the rates associated with one-way quantum communication from Alice to Bob at the same energy. Indeed, it beats the classical capacity of the noiseless quantum channel $I_F(\bar{n}) = (1 + \bar{n})\log_2(1 + \bar{n}) - \bar{n}\log_2\bar{n}$, which can be reached by encoding in Fock states and decoding by photon counting [46,47]. Then, it clearly outperforms the rate $I_S(\bar{n}) = \log_2(1 + 2\bar{n})$ achievable by squeezed states and homodyne detection [48], the rate $I_C^{\rm het}(\bar{n}) = \log_2(1 + \bar{n})$ reachable by coherent states and heterodyne detection [48,49], and finally the rate $I_C(\bar{n}) = \log_2(\sqrt{1 + 4\bar{n}})$ which can be reached by coherent states and homodyne detection [31,32].

V. CONCLUSION

In this paper, we have shown that continuous-variable dense coding can be implemented using an optomechanical cavity as the source of the entanglement. We have considered a high-finesse cavity with a membrane-in-the-middle geometry, i.e., formed by two fixed end mirrors and a perfectly reflecting movable mirror in the middle. The dynamics of the system has been investigated by solving the quantum Langevin equations. After their linearization, we have analyzed the stationary entanglement which can be established between the two output optical modes of the cavity, showing its behavior in terms of the main optomechanical parameters, such as the mechanical damping rates or the laser input powers.

Using the optical entanglement generated by the cavity we have then implemented the protocol of continuous-variable dense coding. We have computed the optomechanical dense coding rate, studying its behavior in terms of the various system parameters, including the input powers, the damping rates, and the quality factor, mass and temperature of the movable mirror. We have shown how this rate approximates the dense coding capacity at low photon numbers ($\bar{n} \simeq 2$), and outperforms the one-way classical capacity of the noiseless quantum channel at higher energies ($\bar{n} > 2$). As a result, we have proven how an optomechanical cavity is able to generate an amount of optical entanglement which is strong enough to implement a standard protocol of quantum information.

ACKNOWLEDGMENTS

We thank M. Woolley for helpful comments. C.W. is supported by NSERC. The work of S.P. has been supported by EPSRC and the Leverhulme Trust. S.B. is grateful for support from the Alexander von Humboldt foundation.

[1] R. Horodecki, P. Horodecki, M. Horodecki, and K. Horodecki, Rev. Mod. Phys. **81**, 865 (2009).
[2] C. Weedbrook, S. Pirandola, R. Garcia-Patron, N. J. Cerf, T. C. Ralph, J. H. Shapiro, and S. Lloyd, Rev. Mod. Phys. **84**, 621 (2012).
[3] C. H. Bennett and S. J. Wiesner, Phys. Rev. Lett. **69**, 2881 (1992).
[4] C. H. Bennett, G. Brassard, C. Crepeau, R. Jozsa, A. Peres, and W. K. Wootters, Phys. Rev. Lett. **70**, 1895 (1993).
[5] A. K. Ekert, Phys. Rev. Lett. **67**, 661 (1991).
[6] M. A. Nielsen and I. L. Chuang, *Quantum Computation and Quantum Information* (Cambridge University Press, Cambridge, 2000).
[7] A. Galindo and M. A. Delgado, Rev. Mod. Phys. **74**, 347 (2002).
[8] P. Kok, W. J. Munro, K. Nemoto, T. C. Ralph, J. P. Dowling, and G. J. Milburn, Rev. Mod. Phys. **79**, 797 (2007).
[9] M. P. Blencowe, Phys. Rep. **395**, 159 (2004).
[10] A. D. Armour, M. P. Blencowe, and K. C. Schwab, Phys. Rev. Lett. **88**, 148301 (2002).
[11] S. Pirandola, S. Mancini, D. Vitali, and P. Tombesi, Phys. Rev. A **68**, 062317 (2003).
[12] S. Pirandola, S. Mancini, D. Vitali, and P. Tombesi, J. Opt. B: Quantum Semiclass. Opt. **5**, S523 (2003).
[13] X. Zou and W. Mathis, Phys. Lett. A **324**, 484 (2004).
[14] S. Pirandola, S. Mancini, D. Vitali, and P. Tombesi, J. Mod. Opt. **51**, 901 (2004).
[15] S. Pirandola, D. Vitali, P. Tombesi, and S. Lloyd, Phys. Rev. Lett. **97**, 150403 (2006).
[16] D. Vitali, S. Gigan, A. Ferreira, H. R. Bohm, P. Tombesi, A. Guerreiro, V. Vedral, A. Zeilinger, and M. Aspelmeyer, Phys. Rev. Lett. **98**, 030405 (2007).
[17] L. Mazzola and M. Paternostro, Nat. Sci. Rep. **1**, 199 (2011).
[18] G. De Chiara, M. Paternostro, and G. M. Palma, Phys. Rev. A **83**, 052324 (2011).
[19] L. Mazzola and M. Paternostro, Phys. Rev. A **83**, 062335 (2011).
[20] B. Rogers, M. Paternostro, G. M. Palma, and G. De Chiara, Phys. Rev. A **86**, 042323 (2012).
[21] M. Paternostro, D. Vitali, S. Gigan, M. S. Kim, C. Brukner, J. Eisert, and M. Aspelmeyer, Phys. Rev. Lett. **99**, 250401 (2007).
[22] S. Barzanjeh, M. Abdi, G. J. Milburn, P. Tombesi, and D. Vitali, Phys. Rev. Lett. **109**, 130503 (2012).
[23] M. Abdi, S. Pirandola, P. Tombesi, and D. Vitali, Phys. Rev. Lett. **109**, 143601 (2012).
[24] A. Xuereb, M. Barbieri, and M. Paternostro, Phys. Rev. A **86**, 013809 (2012).
[25] S. Rips and M. J. Hartmann, Phys. Rev. Lett. **110**, 120503 (2013).
[26] Y. D. Wang and A. A. Clerk, Phys. Rev. Lett. **110**, 253601 (2013).
[27] Sh. Barzanjeh, D. Vitali, P. Tombesi, and G. J. Milburn, Phys. Rev. A **84**, 042342 (2011).
[28] S. A. McGee, D. Meiser, C. A. Regal, K. W. Lehnert, and M. J. Holland, Phys. Rev. A **87**, 053818 (2013).
[29] A. Barenco and A. K. Ekert, J. Mod. Opt. **42**, 1253 (1995).
[30] M. Ban, J. Opt. B: Quantum Semiclass. Opt. **1**, L9 (1999).
[31] S. L. Braunstein and H. J. Kimble, Phys. Rev. A **61**, 042302 (2000).
[32] T. C. Ralph and E. H. Huntington, Phys. Rev. A **66**, 042321 (2002).
[33] J. D. Thompson *et al.*, Nature (London) **452**, 72 (2008).
[34] A. M. Jayich *et al.*, New J. Phys. **10**, 095008 (2008).
[35] C. Genes, A. Mari, P. Tombesi, and D. Vitali, Phys. Rev. A **78**, 032316 (2008).
[36] M. Bhattacharya, H. Uys, and P. Meystre, Phys. Rev. A **77**, 033819 (2008).
[37] C. W. Gardiner and P. Zoller, *Quantum Noise* (Springer, Berlin, 2000).
[38] V. Giovannetti and D. Vitali, Phys. Rev. A **63**, 023812 (2001).
[39] R. Benguria and M. Kac, Phys. Rev. Lett. **46**, 1 (1981).
[40] S. J. van Enk and C. A. Fuchs, Phys. Rev. Lett. **88**, 027902 (2001); D. Vitali, P. Canizares, J. Eschner, and G. Morigi, New J. Phys. **10**, 033025 (2008).
[41] G. Vidal and R. F. Werner, Phys. Rev. A **65**, 032314 (2002); G. Adesso, A. Serafini, and F. Illuminati, *ibid.* **70**, 022318 (2004).
[42] A. Serafini, F. Illuminati, and S. De Siena, J. Phys. B **37**, L21 (2004).
[43] J. D. Teufel *et al.*, Nature (London) **471**, 204 (2011).
[44] M. J. Woolley and A. A. Clerk, Phys. Rev. A **87**, 063846 (2013).
[45] F. Grosshans, N. J. Cerf, J. Wenger, R. Tualle-Brouri, and Ph. Grangier, Quant. Inform. Comp. **3**, 535 (2003).
[46] C. M. Caves and P. D. Drummond, Rev. Mod. Phys. **66**, 481 (1994).
[47] H. P. Yuen and M. Ozawa, Phys. Rev. Lett. **70**, 363 (1993).
[48] Y. Yamamoto and H. A. Haus, Rev. Mod. Phys. **58**, 1001 (1986).
[49] C. Y. She, IEEE Trans. Inf. Theory **IT-14**, 32 (1968).